Hindawi Publishing Corporation
Journal of Nanomaterials
Volume 2014, Article ID 198561, 11 pages
http://dx.doi.org/10.1155/2014/198561

Research Article

Adsorption of Reactive Black 5 on Synthesized Titanium Dioxide Nanoparticles: Equilibrium Isotherm and Kinetic Studies

Majeed A. Shaheed and Falah H. Hussein

Chemistry Department, Faculty of Science, Babylon University, Hilla, Iraq

Correspondence should be addressed to Falah H. Hussein; abohasan_hilla@yahoo.com

Received 29 December 2013; Revised 7 March 2014; Accepted 21 March 2014; Published 15 April 2014

Academic Editor: Arun Kumar

The synthesized titanium dioxide nanoparticles (TiO_2-NPs) were used as adsorbent to remove reactive black 5 (RB 5) in aqueous solution. Various factors affecting adsorption of RB 5 aqueous solutions such as pH, initial concentration, contact time, dose of nanoparticles, and temperature were analyzed at fixed solid/solution ratio. Langmuir and Freundlich isotherms were used as model adsorption equilibrium data. Langmuir isotherm was found to be the most adequate model. The pseudo-first-order, pseudo-second-order, and intraparticle diffusion models were used to describe the adsorption kinetics. The experimental data was fitted to pseudo-second-order kinetics. The thermodynamic parameters such as Gibbs-free energy, enthalpy, and entropy changes were determined. These parameters indicated the endothermic and spontaneity nature of the adsorption. The results demonstrated the fact that the TiO_2-NPs are promising adsorbent for the removal of RB 5 from aqueous solutions.

1. Introduction

In order to remove dyes from wastewaters, there are various methods of development, including chemical oxidation [1], biodegradation [2], electrocoagulation [3], photodegradation [4], solvent extraction [5], ultrafiltration [6], and adsorption [7]. The adsorption technique is the most favorable method for the removal of dyes because of its simple design, easy operation, and relatively simple regeneration [8]. Wastewater industries may contain a variety of organic compounds and toxic substances that exhibit toxic effects for microbial populations and can be toxic and carcinogenic for animals [9].

Azo reactive dyes, which have two azo groups, represent about half of all reactive dyes such as RB 5 (see Figure 1). These types of dyes are known to be toxic, carcinogenic, and mutagenic. Their removal from the environment can result in nonaesthetic pollution. Moreover, these dyes are not easily degraded by conventional aerobic wastewater treatment due to their recalcitrance [10]. Many important sources of environment contamination are synthesis of dye, leather, cosmetics, papers, food processing, pulp mill, pharmaceuticals, and plastics industries [11].

Equilibrium isotherms and kinetics with the presence of methylene blue adsorption onto activated carbon which have been the focus of various studies were used to be prepared from various agricultural wastes such as bamboo [12], coconut husk [13], vetiver roots [14], peach stones [15], rattan sawdust [16], durian shell [17], oil palm fiber [18], coffee husk [19], ground nut shell [20], waste apricot, olive stones [21], hazelnut shell [22], and corncob [23]. Several methods which treat dye wastewater with various biological, chemical, and physical technologies [24, 25] prove to be very useful for environmental purification. Previous studies conducted on the adsorption rate of benzoic acid on cetyl pyridine bromide-modified bentonites fitted a pseudo-second-order kinetics model well ($R^2 = 0.999$). The results were analyzed according to Henry, Langmuir, and Freundlich isotherm model equations. TiO_2 has been extensively studied as one of the superior candidates of semiconductors due to its cheapness, photostability, chemical inertness, nontoxicity, and strong photocatalytic activity [26]. Many methods, such as adsorption, chemical precipitation, ion exchange, membrane processes, biological degradation, chemical oxidation, and solvent extraction have been employed to remove organic

pollutants from aqueous solutions [27]. It is well known that an increase in a plentiful of the surface quality of the TiO_2-NPs is due to the increase of the overall crystallinity and crystal size of nanoparticles which can improve the anchoring geometry of the dye on their surfaces and faster adsorption [28].

Nanomaterials have a higher distortion of surface structure than bulk materials due to their inherent lattice strain. As a result, the surface modifications of TiO_2-NPs are more beneficial for adsorption than that of bulk TiO_2 [30]. Many methods have been employed to fabricate TiO_2-NPs. One of these methods is the metal organic chemical vapor deposition (MOCVD), which is considered a promising technique for producing nanoparticles because of its relative low cost and simplicity of the process [31]. The as-prepared of anatase TiO_2 hollow spheres have a higher surface area; therefore, they showed much higher adsorption and photoreactivity than TiO_2 nanoparticles. In addition, some of hallow spheres which use a sulfonated polystyrene template have very good adsorption and photocatalytic activity [32]. TiO_2 is a very important functional metal oxide material with direct band gap of 3.2 eV at room temperature [33], large specific surface area, and aspect ratio. One-dimensional TiO_2 nanostructures have wide applications in optical, electronic, and photocatalytic fields [34]. The synthesized nanoparticles are attractive for further improvement of the reactivity of TiO_2 as a catalyst. Compared with the other TiO_2 powders, these TiO_2 nanoparticles have several advantages, such as amorphous form, fine particle size with more uniform distribution, and high dispersion in polar solvent, stronger interfacial adsorption, and being environmentally friendly. In the adsorption results, not only the surface area factor should be considered, but also the TiO_2 high ion-exchange ability and the dye cationic character [35]. In our work, 80% of the RB 5 was adsorbed on the surface TiO_2 after one hour of dark stirring conditions. This result is clear evidence of the high RB 5 adsorption capability of adsorbent. Identical adsorbability values were reported in the literature [36]. TiO_2 can be seen as an efficient and cost-effective adsorbent for the removal of pollutants from real wastewaters. The main advantages of the synthesized catalyst for the removal of RB 5 from water and wastewater include a high adsorption rate, capacity, and efficacy, as well as a suitable equilibration time. Furthermore, TiO_2-NPs are available as a no-cost waste and can be used without modifications. Thus, TiO_2-NPs adsorption is environmentally friendly and achieves treatment goals in a simple and low-cost manner. The adsorption emphasizes the engineering applications that govern the actual water purification process, including the fabrication of TiO_2-based adsorbents, process optimization, and economic consideration [37].

Recently, advanced oxidation processes (AOPs) have considerable interest due to their utility in complete elimination of dyes. Most reactive species are generating through AOPs such as hydroxyl radicals that oxidize a broad range of organic pollutants quickly and nonselectively [38, 39]. It is worth mentioning here that the previous studies have not explored this synthesized TiO_2-NPs; thus, this study is considered the first attempt to assess the suitability of this catalyst for engineering applications. In particular, this study aims to determine whether this catalyst delivers better performance in adsorption. It is expected to play a prominent role as an effective adsorbent in competing of the purification processes and economical ways.

2. Experimental Procedure

2.1. Materials. The supplier of reactive black 5 was textile factory (Hilla, Iraq), with formula of $C_{26}H_{21}N_5Na_4O_{19}S_6$, molecular weight of 991.82 g mol^{-1}, and maximum light absorbed wavelength of 597 nm. The synthesized TiO_2-NPs were prepared using sol gel method (from 99.98% absolute EtOH (GCC) and 99.99% $TiCl_4$ (Fluka)).

2.2. Adsorption Experiments. The equilibrium isotherm of RB 5 adsorption on TiO_2-NPs was determined by performing adsorption tests in 250 mL conical flasks. 100 mL of RB 5 dye solutions with different initial concentrations (30, 40, 50, 60, 70, and 80 mg L^{-1}) was placed in each flask. The normal pH of the solutions was 5.5. The prepared TiO_2-NPs of 0.175 g were added to each flask and kept in a shaker of 190 rpm at 30°C for 1 hour to reach equilibrium. The suspensions were sampled at regular intervals. 4 cm^3 of the reaction mixture was collected and centrifuged for 15 min. The supernatant was carefully removed by a syringe with a long pliable needle. This is necessary to remove the fine particles of the catalyst. The supernatant concentrations of RB 5 were analyzed by UV-visible spectrophotometer (PG instruments Ltd., Japan, UV-160A) at maximum wave lengths of 597 nm. The adsorbed amount of RB 5 at equilibrium q_e (mg g^{-1}) was calculated by the following expression:

$$q_e = \frac{(C_o - C_e)\,V}{W}, \tag{1}$$

where C_o and C_e (mg L^{-1}) are the initial and equilibrium concentrations of RB 5 solution, V (L) is the volume of solution, and W (g) is the weight of synthesized TiO_2-NPs used.

A typical preparation procedure is exemplified later in the paper.

2.3. Thermodynamic Experiments. Batch adsorption experiments were performed using 0.175 g of the synthesized TiO_2-NPs with 100 mL of RB 5 aqueous solutions in 250 cm^3 conical flasks. Concentration, pH, and temperature check were determined. The sample was shaken at 120 rpm in a shaking water bath (Memmert GmbH+Co.,KG, Germany). After 60 min desired contact time, suspension was separated by centrifugation. The supernatant solutions for color removal were analyzed by using an UV-vis spectrophotometer (PG instruments Ltd., Japan, UV-160A). The adsorbed amount of RB 5 at equilibrium q_e (mg g^{-1}) was calculated.

3. Results and Discussion

3.1. Adsorption. Adsorption isotherms are important for the description of how adsorbate (RB 5) interacts with an

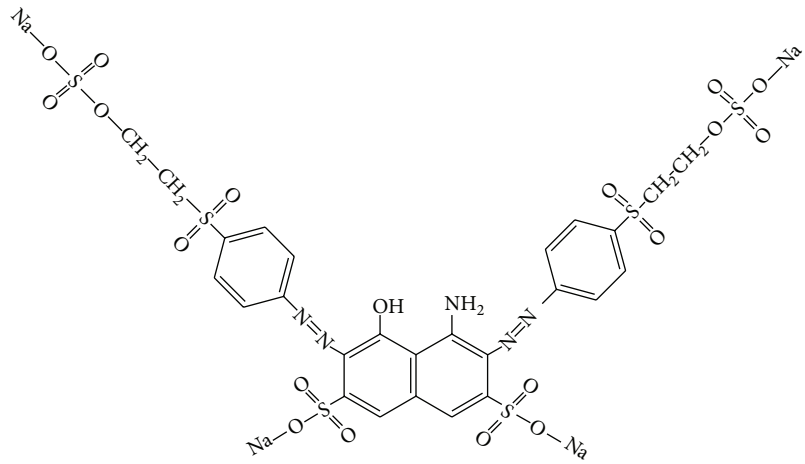

Figure 1: Chemical structure of RB 5 [29].

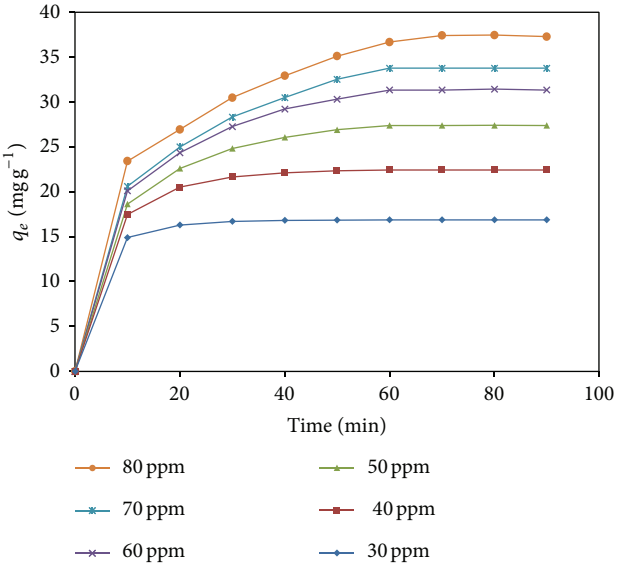

Figure 2: Effect of contact time on adsorption of RB 5 solution.

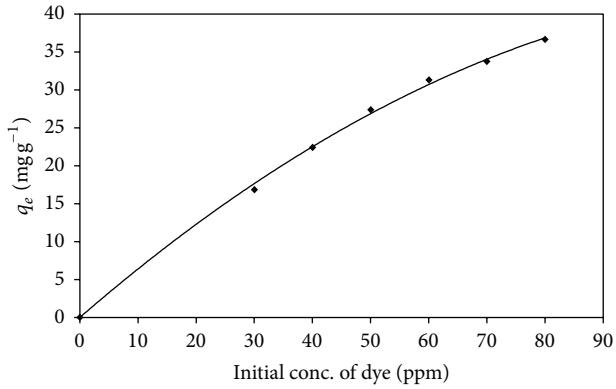

Figure 3: Effect of initial concentration on amount of adsorption of RB 5 dye.

adsorbent (TiO_2-NPs) and are also critical in optimizing the use of adsorbent. Thus, the correlation of experimental equilibrium data using either a theoretical or empirical equations is essential for adsorption data interpretation and prediction. Several mathematical models can be used to describe experimental data of adsorption isotherms. Five famous isotherm equations, namely, the Langmuir, Freundlich, pseudo-first-order, pseudo-second-order, and intraparticle diffusion model, were applied to fit the experimental equilibrium isotherm data of RB 5 adsorption on the prepared TiO_2-NPs.

3.2. Fundamental Parameters in Adsorption

3.2.1. Effect of Contact Time. The effect of contact time on adsorption capacity of TiO_2-NPs for RB 5 at different initial concentrations of RB 5 is shown in Figure 2. The results indicate that the adsorbed amount of RB 5 increases with the increase of contact time. The adsorption approximately reached equilibrium in about 1 hour. The maximum adsorbed amount of 16.87, 22.43, 27.38, 31.33, 33.76, and 36.67 mg g^{-1} was obtained at 30, 40, 50, 60, 70, and 80 mg L^{-1} initial RB 5 concentration, respectively; one hour contact time; normal pH value 5.5; and 1.75 g L^{-1} adsorbent dose. These results also show that rapid increase in adsorbed amount of RB 5 was achieved during the first 10 minutes. Similar results for the removal of hazardous contaminants from wastewater were reported [40]. The fast adsorption at the initial stage may be due to the higher driving force making fast transfer of RB 5 to the surface of TiO_2-NPs, the availability of the uncovered surface area, and the remaining active sites on the adsorbent [41].

3.2.2. Effect of Initial Concentration of RB 5 Dye. Six different concentrations of 30, 40, 50, 60, 70, and 80 mg L^{-1} for RB 5 were selected to investigate the effect of initial concentration of dye onto the synthesized TiO_2-NPs. The amounts of dye

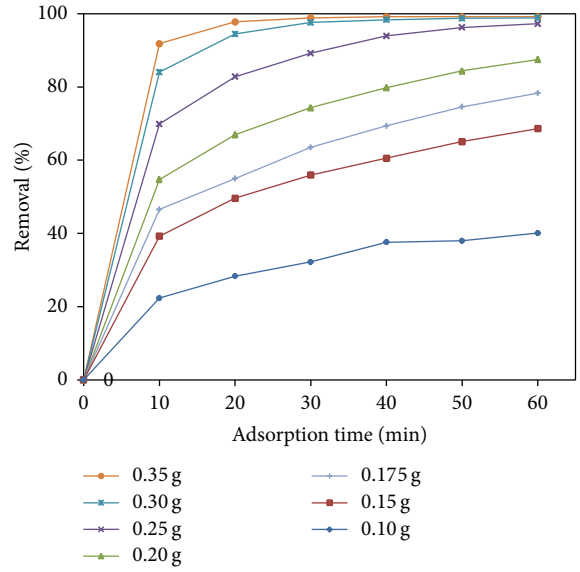

Figure 4: Effect of TiO_2-NPs dosage on removal percentage of RB 5 (initial concentration of RB 5 = 80 mg L^{-1}, pH 5.5, contact time = 1 h).

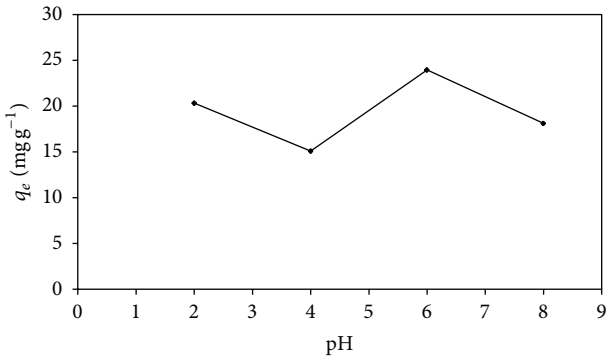

Figure 5: Effect of pH on adsorption of RB 5 solution.

molecules adsorbed at equilibrium and pH 5.5 are graphed in Figure 3. With the initial increase of the concentration of RB 5 from 30 to 80 mg L^{-1}, the removal of dye molecules adsorbed by adsorbent decreases from 98.04 to 80.21% after one hour of adsorption time. These results correspond to the adsorption of nitrate from aqueous solution using modified rice husk [42].

3.2.3. Effect of Adsorbent Dosage. The effect of adsorbent dosage on the adsorption of RB 5 is shown in Figure 4. The percent removal increases from 40.06 to 99.16% by increasing the adsorbent dosage from 0.1 to 0.35 g after one hour of adsorption time. It is apparent from this figure that, by increasing the catalyst amount, the adsorption efficiency increases, but adsorption density and the amount adsorbed per unit mass decrease. It is easily understood that the number of available adsorption sites increases by increasing the adsorbent amount, but the drop in adsorption capacity is basically due to the sites remaining unsaturated during the adsorption process. If the active sites are available, the pollutant left in the system will continuously be adsorbed. In other words, the increase with TiO_2-NPs dosage of the amount of dye adsorbed was caused by the availability of more surface area of the TiO_2-NPs. Direct evidence of TiO_2-NPs entanglement was not clear and unexpected. However, similar observations can be found in the literature [43–46].

3.2.4. Effect of pH. The adsorption of the RB 5 onto an adsorbent generally varies with pH because pH changes the radius of hydrolyzed cation and the charge of the adsorbent surface. Therefore, in this study, the adsorption of RB 5 dye onto the prepared TiO_2-NPs in our lab was studied as a function of pH. The pH values of RB 5 solutions were adjusted as 2.0, 4.0, 6.0, and 8.0. The relationship between initial pH and the amounts of dye adsorbed on the TiO_2-NPs for the initial solution concentration of 70 mg L^{-1} at 30°C and a contact time of 60 min is illustrated in Figure 5. pH change affects the adsorption quantity of organic pollutants and the ways of adsorption on the surface of catalyst. As a result, the adsorption efficiency will greatly be influenced by pH changes which can be explained with the protonation or unprotonation of the functional groups on the surface of TiO_2 as well as the dye. When initial pH values of solutions are increased from 2.0 to 8.0, the amounts of adsorbed dye per unit mass of adsorbent are changed. For example, the amounts of dye molecules adsorbed dye per adsorbent decrease from 20.32 to 15.08 mg g^{-1} when the pH value increases from 2.0 to 4.0. As seen in this figure, pH 6 is a value for the maximum adsorption of RB 5. A rising in the pH closes to 6.0 gives the maximum adsorption capacity. In this point, pH was called the zero point charge (Z.P.C). Hussein [47] reported that the zero point charge for commercial TiO_2 (Degussa P25) is equal to 6.25. Also, when the pH values of solutions were continuously increased from 6.0 to 8.0, the amounts of dye molecules adsorbed per unit adsorbent decrease from 23.95 to 18.11 mg g^{-1}. These results indicate that the adsorbed amount of RB 5 was strongly dependent on pH of solution because the reaction takes place on the surface of synthesized catalyst. The concept could be explained as follows: the increase of the pH solution makes the surface of catalyst negatively charged by adsorbed hydroxyl ions and the decrease of the pH solution makes it positively charged by adsorbed hydrogen ions. Both the acidic and basic media leave an inverse impact on the adsorption efficiency because of the change of electrostatic forces between surface catalyst and dye molecules.

3.2.5. Effect of Temperature. The uptake of dye solution was increased with the rise in temperature from 5 to 30°C as shown in Figure 6. Equilibrium time was found to be reached in 60 min, at pH 5.5, and 50 mg L^{-1} of dye solution. The adsorption kinetics depends on the surface area of the adsorbent. The adsorption which increased with temperature indicates that the mobility of dye molecules increased with temperature, as did the number of dye molecules that interact with the active sites at TiO_2-NPs. Moreover, the viscosity of dye solution reduces with the rise in temperature, increasing

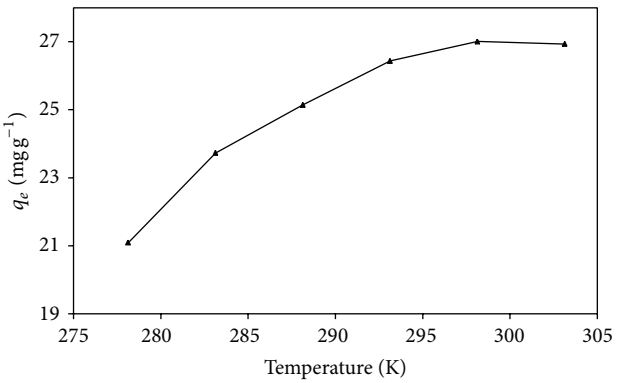

Figure 6: Effect of temperature on adsorption of RB 5 solution.

the rate of diffusion of dye molecules. These results also showed that the adsorption process was endothermic and spontaneous in nature. These results are in agreement with application of acidic treated pumice for the removal of azo dye from aqueous solution [48].

3.3. Analysis of Adsorption Kinetics. Numerous adsorption processes have been studied during the past 25 years. The diffusion control, mass transfer, chemical reactions, and particle diffusion are different kinds of mechanisms related to adsorption processes. The pseudo-first-order kinetic model, pseudo-second-order kinetic model, and intraparticle diffusion model were used for testing dynamic experimental data at 0.175 g of adsorbent and the different initial concentrations of RB 5 were 30, 40, 50, 60, 70, and 80 mg L^{-1} in the normal pH 5.5. The pseudo-first-order kinetic model of Lagergren is given as [49]

$$\ln(q_e - q_t) = \ln(q_e) - k_1 t, \tag{2}$$

where q_e and q_t (mg g^{-1}) are the amount of RB 5 adsorbed at equilibrium and at time t (min), respectively, and k_1 (min^{-1}) is the adsorption rate constant.

The pseudo-second-order kinetic model can be expressed as [50]

$$\frac{t}{q_t} = \frac{1}{k_2 q_e^2} + \frac{t}{q_e}, \tag{3}$$

where k_2 (g mg^{-1} min^{-1}) is the rate constant of second-order equation.

The initial adsorbent rate h (mg g^{-1} min^{-1}) can be determined from k_2 and q_e values using the following equation:

$$h = k_2 q_e^2. \tag{4}$$

The intraparticle diffusion model can be described as [51]

$$q_t = k_i t^{1/2}, \tag{5}$$

where q_t is the amount of dye adsorbed at time t (min) and k_i is the intraparticle diffusion rate constant (mg g^{-1} min$^{-1/2}$).

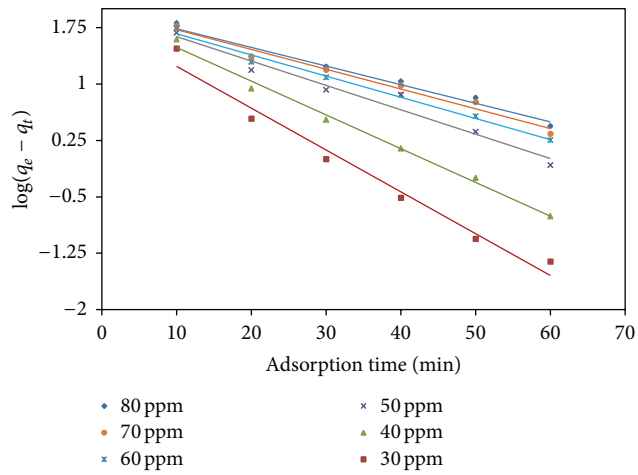

Figure 7: Pseudo-first-order kinetic model.

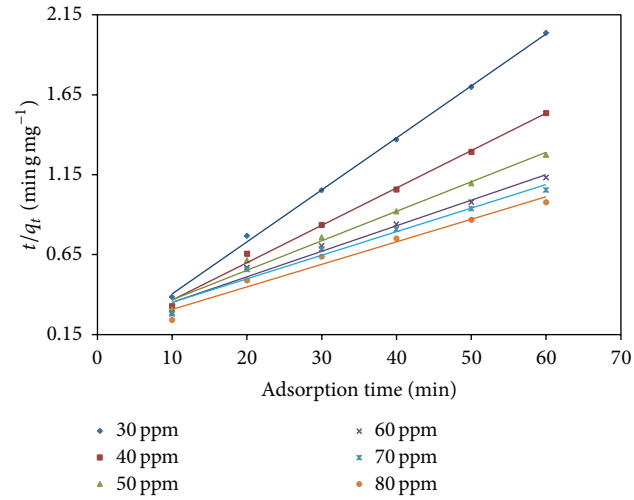

Figure 8: Pseudo-second-order kinetic model.

Moreover, the validity of these models was determined by calculating the standard deviation (R.S.D%) using

$$\text{R.S.D\%} = \sqrt{\frac{\sum\left[\left(q_{\text{exp}} - q_{\text{cal}}\right)/q_{\text{exp}}\right]^2}{n-1}} \times 100\%, \tag{6}$$

where subscripts exp and cal refer to the experimental and calculated data and n is the number of data points.

In adsorption process, there are two criteria, namely, the regression coefficients and predicted q_e values that assess the validity of the order of adsorption [52]. The validities of these three kinetic models for all concentrations are checked and depicted in Figures 7, 8, and 9. The values of the parameters, correlation coefficient, and standard deviation obtained from these three kinetic models are all listed in Table 1. Among these, Figure 8 shows a good agreement with pseudo-second-order kinetic model. Table 1 presents the coefficients and R.S.D% of the pseudo-first- and second-order adsorption kinetic models and the intraparticle diffusion model. The values of R^2 for pseudo-second-order

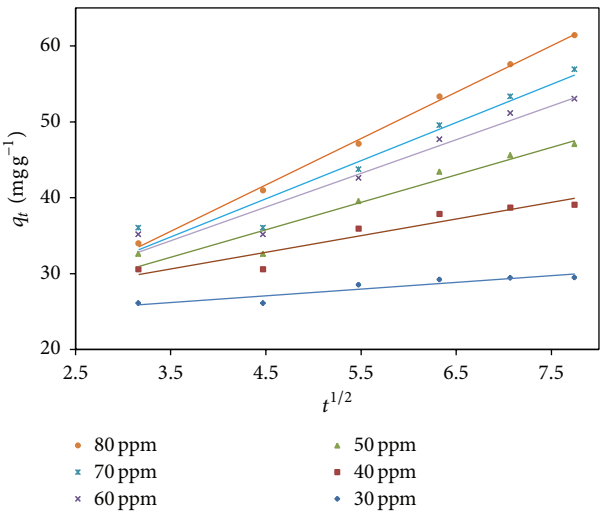

Figure 9: Intraparticle diffusion model.

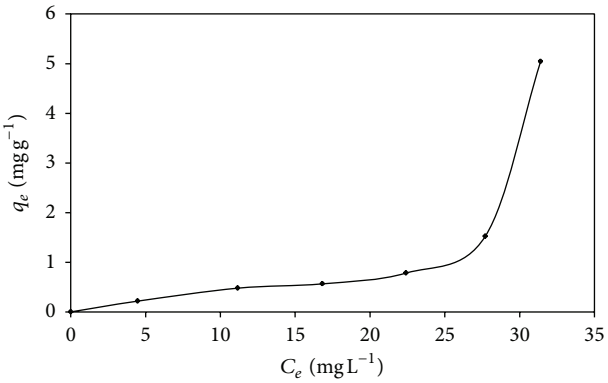

Figure 10: Adsorption isotherm of RB 5 dye in presence of TiO_2-NPs.

kinetic model are extremely high (all greater than 0.9989), but R.S.D values of the pseudo-second-order are smaller than those of the pseudo-first-order and the intraparticle diffusion model. Hence, this study suggests that the pseudo-second-order model better represents the adsorption kinetics. Consequently, the description of adsorption process could be the best by the pseudo-second-order kinetic. This also implies that the rate-limiting step may be the chemical adsorption. A similar phenomenon has been observed in the literature [53, 54]. The values of the pseudo-second-order rate constant, k_2, were found to decrease from 1.32×10^{-2} to 1.2×10^{-3} g mg^{-1} min^{-1}, for an increase in the concentration solution of dye solution from 30 to 80 g L^{-1}.

Table 2 shows the values of adsorption rate constant at the following concentrations (30, 40, 50, and 60 mg L^{-1}), K_{ad} was found to increase from 19.142, 9.736, 1.611, and 0.435 to 130.857, 43.238, 9.859, and 1.370 L g^{-1}, for an increase in the solution temperature of 278.14 to 303.14 K, respectively.

3.4. Analysis of Adsorption Isotherm. The relationship between the amount of RB 5 dye adsorbed onto the adsorbent

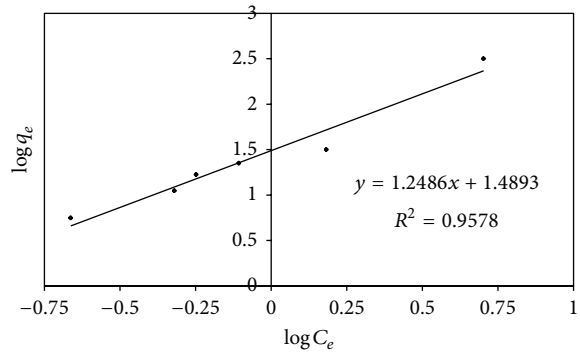

Figure 11: Freundlich isotherm.

surface and the remaining RB 5 concentration in the aqueous phase at equilibrium can be observed by the equilibrium adsorption isotherm analysis as shown in the investigation of the effect of initial concentration of dye. This relationship which is shown in Figure 10 indicates that the adsorption capacity RB 5 dye on the surface of TiO_2-NPs increases with the equilibrium concentration of dye solution, progressively reaching saturation of the adsorbent. Adsorption isotherm curve indicates that adsorption phenomenon is represented by isotherms of type L which represent a monolayer adsorption until the saturation of active sites. The higher dye adsorption value reveals that the synthesized TiO_2-NPs are well interconnected and the electrons are efficiently transported through the particles. This is consistent with the work reported by Kathirvel et al. [55].

The study employed the Langmuir and Freundlich models to describe the equilibrium adsorption. The expression of the Freundlich model [56] is

$$q_e = K_f C_e^{1/n}. \tag{7}$$

In logarithmic form,

$$\ln q_e = \ln K_f + \frac{1}{n} \ln C_e, \tag{8}$$

where q_e is the amount of RB 5 adsorbed at equilibrium time (mg g^{-1}) and C_e is the equilibrium concentration of the dye solution (mg L^{-1}). K_f(mg g^{-1})/(mg L^{-1})$^{1/n}$ and n are Freundlich isotherm constants which indicate capacity and intensity of the adsorption, respectively.

Freundlich [$R^2 = 0.9578$] is not as adequate as Langmuir model [$R^2 = 0.9724$]. The values of K_f and n were calculated from the slope and intercept of the plot log q_e versus log C_e (Figure 11). The values of K_f and n obtained are shown in Table 3. From n value physical adsorption is unfavorable because the value of n is not in the range $1 < n < 10$ [57].

The Langmuir isotherm is expressed as [58]

$$\frac{1}{q_e} = \frac{1}{q_m} + \frac{1}{K_L q_m C_e}, \tag{9}$$

where q_m (mg g^{-1}) is the maximum amount of RB 5 per unit weight of TiO_2-NPs to form complete monolayer coverage on

Table 1: Adsorption parameters.

Kinetic parameters for RB 5 adsorption on TiO_2-NPs					
Pseudo first order model					
C_o (ppm)	q_e, exp (mg g^{-1})	q_e, cal (mg g^{-1})	k_1 min^{-1}	R^2	R.S.D (%)
30	16.8695	0.5828	0.0240	0.9754	7.529
40	22.4347	0.6609	0.0260	0.9918	10.020
50	27.3788	0.6704	0.0280	0.9642	12.233
60	31.3292	0.6679	0.0320	0.9888	14.001
70	33.7639	0.9855	0.0440	0.9784	15.087
80	36.6708	0.6855	0.0550	0.9724	16.391
Pseudo-second-order model					
C_o (ppm)	q_e, exp (mg g^{-1})	q_e, cal (mg g^{-1})	k_2 (g mg^{-1} min^{-1})	R^2	R.S.D (%)
30	16.8695	30.7692	0.0132	0.9989	6.729
40	22.4347	42.7350	0.0041	0.9951	9.181
50	27.3788	54.3478	0.0019	0.9863	11.356
60	31.3292	62.5000	0.0013	0.9792	13.119
70	33.7639	68.0272	0.0011	0.9704	14.199
80	36.6708	70.9219	0.0012	0.9720	15.535
Intraparticle diffusion model					
C_o (ppm)	q_e, exp (mg g^{-1})	C (mg g^{-1})	k_{id} (mg g^{-1} min$^{-1/2}$)	R^2	R.S.D (%)
30	16.8695	23.0690	0.8879	0.8629	6.933
40	22.4348	22.9300	2.1929	0.8962	9.576
50	27.3789	19.5110	3.6157	0.9317	11.926
60	31.3292	18.8080	4.4369	0.9362	13.742
70	33.7639	17.2540	5.0252	0.9379	14.871
80	36.6708	14.1950	6.1106	0.9979	16.227

Table 2: Adsorption constants at different concentrations and temperatures.

Temperature (K)	Adsorption constant (K_{ad})			
	At 30 ppm	At 40 ppm	At 50 ppm	At 60 ppm
278.15	19.142	9.736	1.611	0.435
283.15	32.285	13.263	2.798	0.656
288.15	43.238	19.648	4.190	0.749
293.15	78.285	34.476	7.069	0.804
298.15	98.000	52.000	9.380	1.120
303.15	130.857	43.238	9.859	1.370

Table 3: Adsorption constants for Langmuir and Freundlich.

Isotherm parameter for RB 5 adsorption on TiO_2-NPs		
Isotherm	Parameter	Value
Langmuir	q_m (mg g^{-1})	88.495
	K_L (L mg^{-1})	0.3210
	R^2	0.9629
Freundlich	K_F	2.2190
	n	0.8009
	R^2	0.9578

the surface bound at high equilibrium RB 5 concentration C_e and K_L is Langmuir constant related to the affinity of binding sites (L mg^{-1}). q_m represents a particle limiting adsorption capacity when the surface is fully covered with dye molecules and assists in the comparison of adsorption performance. q_m and K_L are calculated from the slope and intercept of the straight line of the plot of $1/q_e$ versus $1/C_e$ as shown in Figure 12.

Table 4: Relation of R_L with type of isotherm.

Value of R_L	Type of isotherm
$R_L > 1$	Unfavorable
$R_L = 1$	Linear
$0 < R_L < 1$	Favorable
$R_L = 0$	Irreversible

Parameters of the Langmuir and Freundlich isotherms are computed in Table 4. Langmuir isotherm fits quite well with the experimental adsorption data correlation coefficient (R^2), whereas the low R^2 shows poor agreement of the Freundlich isotherm with the experimental data. Calculated maximum capacities (q_m) are close to maximum capacities obtained at equilibrium (Table 3).

Furthermore, the essential characteristic of the Langmuir isotherm can be expressed by a dimensionless separation factor called equilibrium parameter [59] R_L. It is also evaluated in this study and is determined from the relation

$$R_L = \frac{1}{1 + K_L C_e}, \quad (10)$$

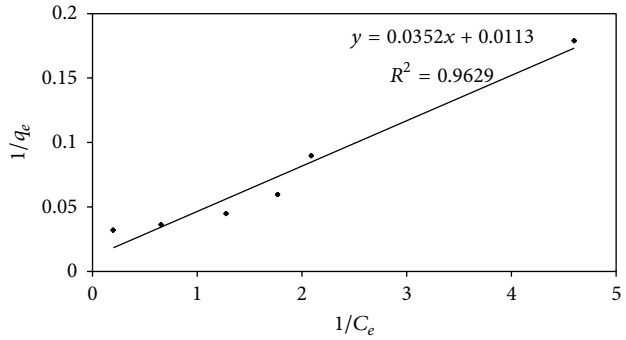

Figure 12: Langmuir isotherm.

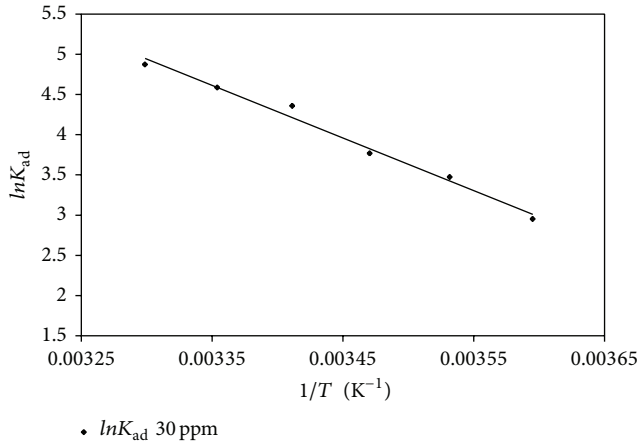

Figure 13: The plot of $\ln K_{ad}$ versus $1/T$ for the determination of thermodynamic parameters.

where K_L is the Langmuir constant ($mL\,g^{-1}$) and C_e is the initial dye concentration ($mg\,L^{-1}$). Parameter R_L indicates the shape of isotherm as shown in Table 4.

R_L value between 0 and 1 indicates a favorable adsorption. The values of R_L between 0 and 1 indicate a favorable chemical adsorption. The results show that, for Langmuir isotherm, the value of R_L is found to be 0.042605, suggesting that the prepared TiO_2-NPs are favorable for adsorption of RB 5 under the conditions used in this study.

The fact that the Langmuir isotherm fits the experimental data very well may be due to homogenous distribution of active sites on the TiO_2-NPs surface, since the Langmuir equation assumes that the surface of catalyst is homogeneous [60].

3.5. Analysis of Adsorption Thermodynamic. The thermodynamic parameters should be properly evaluated because they provide in depth information regarding the inherent energetic changes associated with adsorption. Free energy of adsorption (ΔG°), enthalpy (ΔH°), and entropy (ΔS°) changes were calculated in this study to predict the process of adsorption. Determination of the thermodynamic parameters is independent of the Langmuir equilibrium adsorption constant, K_L. The van't Hoff equation is used to evaluate the variation of equilibrium adsorption constant with temperature [61]. The integrated form of this equation is given as

$$\ln K_{\text{ad}} = -\frac{\Delta H^\circ}{RT} + \frac{\Delta S^\circ}{R}. \tag{11}$$

Gibbs free energy change of adsorption (ΔG°) was calculated as −6.815, −8.166, −9.009, −10.610, −11.346 and −12.264 k J mol^{-1}at 278.14, 283.14, 288.14, 293.14, 298.14 and 303.14 K, respectively onto the synthesized TiO_2-NPs at concentration was 30 $mg\,L^{-1}$. The negative ΔG° values indicated that the adsorption of RB 5 onto TiO2-NPs was thermodynamically feasible and spontaneous. The enthalpy (ΔH°) and entropy (ΔS°) changes were determined as 54.248 k J mol^{-1} and 26.509 × 10^3 J mol^{-1} K^{-1} from $\ln K_{ad}$ versus $1/T$ plot (Figure 13). The positive value of ΔH° confirmed the endothermic character of the adsorption process. The positive values of ΔS° also revealed the increase of randomness at the solid-liquid interface during the adsorption of RB 5 onto the TiO_2-NPs. The low value of ΔS° indicated that no remarkable change on entropy occurs. Similar results on RB 5 as compared to other materials [62] indicated that the adsorption of RB 5 was feasible, spontaneous, and endothermic. Thus results show that the adsorbents can be used for the treatment of aqueous solutions as an alternative low-cost adsorbent.

4. Conclusions

The synthesized TiO_2-NPs are a well-known adsorbent that can be used to remove azo dyes such as RB 5. Among the kinetic models, the pseudo-second-order kinetic model was considered the best to explain the behavior of the adsorption process because the average R^2 of pseudo-second-order is the highest among other models (pseudo-first-order average R^2 = 0.9739, pseudo-second-order average R^2 = 0.98545, and intraparticle diffusion average R^2 = 0.9304). The extent of RB 5 adsorption on TiO_2 increases along with an increase of initial RB 5 concentration. Freundlich and Langmuir isotherm models have been found to be suitable for the description of adsorption. The synthesized catalyst has been found to have a Langmuir monolayer adsorption capacity of 88.495 $mg\,g^{-1}$ at normal pH 5.5 and 30°C. The Langmuir model fitted the experimental data better than Freundlich model indicating that the adsorption tends to monolayer adsorption. The dimensionless separation factor R_L confirms that the adsorption process certainly involves chemical adsorption. The pH of the zero point charge (pH_{zpc}) for the adsorption process was determined to be 6. The results demonstrated that the prepared TiO_2-NPs are a promising adsorbent for the removal of RB 5 dye from aqueous solutions. From the results of thermodynamic parameters, the negative ΔG° values indicated that the adsorption of RB 5 onto TiO_2-NPs was thermodynamically feasible and spontaneous. The kinetic studies showed that the contact time was suitable for technological applications. Consequently, fundamentally the outlook is promising that the prepared

TiO_2-NPs have higher potential of removing the most significant amounts of azo dyes from aqueous solutions. Moreover, the adsorbate and adsorbent ratio provides an economical way to produce expensive semiconductor material support and it is convenient for the detoxification of pollutants.

Conflict of Interests

The authors declare that there is no conflict of interests regarding the publication of this paper.

Acknowledgments

This paper was supported by Advanced Lab of Physical Chemistry, University of Babylon, Hilla, Iraq. The authors also acknowledge Dr. Fadhil Mohsen's technical assistance and the support they received from the Iraqi Ministry of Science and Technology.

References

[1] L. Chengtang, X. Hui, L. Huaming, L. Ling, X. Li, and Y. Zhixiang, "Efficient degradation of methylene blue dye by catalytic oxidation using the $Na_8Nb_6O_{19}{\cdot}13H_2O/H_2O_2$ system," *Korean Journal of Chemical Engineering*, vol. 28, no. 4, pp. 1126–1132, 2011.

[2] S. A. Ong, E. Toorisaka, M. Hirata, and T. Hano, "Biodegradation of redox dye methylene blue by up-flow anaerobic sludge blanket reactor," *Journal of Hazardous Materials B*, vol. 124, no. 1–3, pp. 88–94, 2005.

[3] A. K. Golder, N. Hridaya, A. N. Samanta, and S. Ray, "Electrocoagulation of methylene blue and eosin yellowish using mild steel electrodes," *Journal of Hazardous Materials*, vol. 127, no. 1–3, pp. 134–140, 2005.

[4] I. Fatimah, S. Wang, and D. Wulandari, "ZnO/montmorillonite for photocatalytic and photochemical degradation of methylene blue," *Applied Clay Science*, vol. 53, no. 4, pp. 553–560, 2011.

[5] G. Muthuraman, T. T. Teng, C. P. Leh, and I. Norli, "Extraction and recovery of methylene blue from industrial wastewater using benzoic acid as an extractant," *Journal of Hazardous Materials*, vol. 163, no. 1, pp. 363–369, 2009.

[6] M. Bielska and K. Prochaska, "Dyes separation by means of cross-flow ultrafiltration of micellar solutions," *Dyes and Pigments*, vol. 74, no. 2, pp. 410–415, 2007.

[7] A. M. M. Vargas, A. L. Cazetta, M. H. Kunita, T. L. Silva, and V. C. Almeida, "Adsorption of methylene blue on activated carbon produced from flamboyant pods (Delonix regia): study of adsorption isotherms and kinetic models," *Chemical Engineering Journal*, vol. 168, no. 2, pp. 722–730, 2011.

[8] A. L. Ahmad, M. M. Loh, and J. A. Aziz, "Preparation and characterization of activated carbon from oil palm wood and its evaluation on methylene blue adsorption," *Dyes and Pigments*, vol. 75, no. 2, pp. 263–272, 2007.

[9] X. Han, W. Wang, and X. Ma, "Adsorption characteristics of methylene blue onto low cost biomass material lotus leaf," *Chemical Engineering Journal*, vol. 171, no. 1, pp. 1–8, 2011.

[10] S. Chatterjee, S.-R. Lim, and S. H. Woo, "Removal of reactive black 5 by zero-valent iron modified with various surfactants," *Chemical Engineering Journal*, vol. 160, no. 1, pp. 27–32, 2010.

[11] Y. Yao, F. Xu, M. Chen, Z. Xu, and Z. Zhu, "Adsorption behavior of methylene blue on carbon nanotubes," *Bioresource Technology*, vol. 101, no. 9, pp. 3040–3046, 2010.

[12] B. H. Hameed, A. T. M. Din, and A. L. Ahmad, "Adsorption of methylene blue onto bamboo-based activated carbon: kinetics and equilibrium studies," *Journal of Hazardous Materials*, vol. 141, no. 3, pp. 819–825, 2007.

[13] I. A. W. Tan, A. L. Ahmad, and B. H. Hameed, "Adsorption of basic dye on high-surface-area activated carbon prepared from coconut husk: equilibrium, kinetic and thermodynamic studies," *Journal of Hazardous Materials*, vol. 154, no. 1–3, pp. 337–346, 2008.

[14] S. Altenor, B. Carene, E. Emmanuel, J. Lambert, J.-J. Ehrhardt, and S. Gaspard, "Adsorption studies of methylene blue and phenol onto vetiver roots activated carbon prepared by chemical activation," *Journal of Hazardous Materials*, vol. 165, no. 1–3, pp. 1029–1039, 2009.

[15] A. A. Attia, B. S. Girgis, and N. A. Fathy, "Removal of methylene blue by carbons derived from peach stones by H_3PO_4 activation: batch and column studies," *Dyes and Pigments*, vol. 76, no. 1, pp. 282–289, 2008.

[16] B. H. Hameed, A. L. Ahmad, and K. N. A. Latiff, "Adsorption of basic dye (methylene blue) onto activated carbon prepared from rattan sawdust," *Dyes and Pigments*, vol. 75, no. 1, pp. 143–149, 2007.

[17] T. C. Chandra, M. M. Mirna, Y. Sudaryanto, and S. Ismadji, "Adsorption of basic dye onto activated carbon prepared from durian shell: studies of adsorption equilibrium and kinetics," *Chemical Engineering Journal*, vol. 127, no. 1–3, pp. 121–129, 2007.

[18] I. A. W. Tan, B. H. Hameed, and A. L. Ahmad, "Equilibrium and kinetic studies on basic dye adsorption by oil palm fibre activated carbon," *Chemical Engineering Journal*, vol. 127, no. 1–3, pp. 111–119, 2007.

[19] L. C. A. Oliveira, E. Pereira, I. R. Guimaraes et al., "Preparation of activated carbons from coffee husks utilizing $FeCl_3$ and $ZnCl_2$ as activating agents," *Journal of Hazardous Materials*, vol. 165, no. 1–3, pp. 87–94, 2009.

[20] N. Kannan and M. M. Sundaram, "Kinetics and mechanism of removal of methylene blue by adsorption on various carbons—a comparative study," *Dyes and Pigments*, vol. 51, no. 1, pp. 25–40, 2001.

[21] M. N. Alaya, M. A. Hourieh, A. M. Youssef, and F. El-Sejariah, "Adsorption properties of activated carbons prepared from olive stones by chemical and physical activation," *Adsorption Science and Technology*, vol. 18, no. 1, pp. 27–42, 2000.

[22] A. Aygün, S. Yenisoy-Karakaş, and I. Duman, "Production of granular activated carbon from fruit stones and nutshells and evaluation of their physical, chemical and adsorption properties," *Microporous and Mesoporous Materials*, vol. 66, no. 2-3, pp. 189–195, 2003.

[23] R. L. Tseng, S. K. Tseng, and F. C. Wu, "Preparation of high surface area carbons from Corncob with KOH etching plus CO_2 gasification for the adsorption of dyes and phenols from water," *Colloids and Surfaces A: Physicochemical and Engineering Aspects*, vol. 279, no. 1–3, pp. 69–78, 2006.

[24] T. Robinson, G. McMullan, R. Marchant, and P. Nigam, "Remediation of dyes in textile effluent: a critical review on current treatment technologies with a proposed alternative," *Bioresource Technology*, vol. 77, no. 3, pp. 247–255, 2001.

[25] J. He, S. Hong, L. Zhang, F. Gan, and Y. S. Ho, "Equilibrium and thermodynamic parameters of adsorption of methylene blue

onto rectorite," *Fresenius Environmental Bulletin A*, vol. 19, no. 11, pp. 2651–2656, 2010.

[26] Z. Xie, Y. Zhang, X. Liu et al., "Visible light photoelectrochemical properties of N-doped TiO_2 nanorod arrays from TiN," *Journal of Nanomaterials*, vol. 2013, Article ID 930950, 8 pages, 2013.

[27] X. Xin, J. Yang, R. Feng et al., "Preparation, characterization and adsorption performance of cetyl pyridine bromide modified bentonites," *Journal of Inorganic and Organometallic Polymers and Materials*, vol. 22, no. 1, pp. 42–47, 2012.

[28] H. Nishikiori, W. Qian, M. A. El-Sayed, N. Tanaka, and T. Fujii, "Change in titania structure from amorphousness to crystalline increasing photoinduced electron-transfer rate in dye-titania system," *Journal of Physical Chemistry C*, vol. 111, no. 26, pp. 9008–9011, 2007.

[29] M. Cerón-Rivera, M. M. Dávila-Jiménez, and M. P. Elizalde-González, "Degradation of the textile dyes basic yellow 28 and Reactive black 5 using diamond and metal alloys electrodes," *Chemosphere*, vol. 55, no. 1, pp. 1–10, 2004.

[30] C. Burda, Y. Lou, X. Chen, A. C. S. Samia, J. Stout, and J. L. Gole, "Enhanced nitrogen doping in TiO_2 nanoparticles," *Nano Letters*, vol. 3, no. 8, pp. 1049–1051, 2003.

[31] S. Abdul Rashid, S. H. Othman, T. I. Mohd Ghazi, and N. Abdullah, "Fe-doped TiO_2 nanoparticles produced via MOCVD: synthesis, characterization, and photocatalytic activity," *Journal of Nanomaterials*, vol. 2011, Article ID 571601, 11 pages, 2011.

[32] Z. Zhou, Y. Ding, X. Zu, and Y. Deng, "ZnO spheres and nanorods formation: their dependence on agitation in solution synthesis," *Journal of Nanoparticle Research*, vol. 13, no. 4, pp. 1689–1696, 2011.

[33] S. Khan, I. A. Qazi, I. Hashmi, M. A. Awan, and Z. Najum-us-Sehar Sadaf, "Synthesis of silver-doped titanium TiO_2 powder-coated surfaces and its ability to inactivate *Pseudomonas aeruginosa* and *Bacillus subtilis*," *Journal of Nanomaterials*, vol. 2013, Article ID 531010, 8 pages, 2013.

[34] Y. Liu, Y. Jiao, F. Qu, L. Gong, and X. Wu, "Facile synthesis of template-induced SnO_2 nanotubes," *Journal of Nanomaterials*, vol. 2013, Article ID 610964, 6 pages, 2013.

[35] E. K. Ylhäinen, M. R. Nunes, A. J. Silvestre, and O. C. Monteiro, "Synthesis of titanate nanostructures using amorphous precursor material and their adsorption/photocatalytic properties," *Journal of Materials Science*, vol. 47, no. 10, pp. 4305–4312, 2012.

[36] J. Huang, Y. Cao, Z. Deng, and H. Tong, "Formation of titanate nanostructures under different NaOH concentration and their application in wastewater treatment," *Journal of Solid State Chemistry*, vol. 184, no. 3, pp. 712–719, 2011.

[37] C. Wang, H. Liu, and Y. Qu, "TiO_2-based photocatalytic process for purification of polluted water: bridging fundamentals to applications," *Journal of Nanomaterials*, vol. 2013, Article ID 319637, 14 pages, 2013.

[38] S. Das, P. V. Kamat, S. Padmaja, V. Au, and S. A. Madison, "Free radical induced oxidation of the azo dye acid yellow 9," *Journal of the Chemical Society*, vol. 2, no. 6, pp. 1219–1223, 1999.

[39] Y. Yang, D. T. Wyatt II, and M. Bahorsky, "Decolorization of dyes using UV/H_2O_2 photochemical oxidation," *Textile Chemist and Colorist*, vol. 30, no. 4, pp. 27–35, 1998.

[40] M. Toor and B. Jin, "Adsorption characteristics, isotherm, kinetics, and diffusion of modified natural bentonite for removing diazo dye," *Chemical Engineering Journal*, vol. 187, pp. 79–88, 2012.

[41] M. K. Aroua, S. P. P. Leong, L. Y. Teo, C. Y. Yin, and W. M. A. W. Daud, "Real-time determination of kinetics of adsorption of lead(II) onto palm shell-based activated carbon using ion selective electrode," *Bioresource Technology*, vol. 99, no. 13, pp. 5786–5792, 2008.

[42] R. Katal, M. S. Baei, H. T. Rahmati, and H. Esfandian, "Kinetic, isotherm and thermodynamic study of nitrate adsorption from aqueous solution using modified rice husk," *Journal of Industrial and Engineering Chemistry*, vol. 18, no. 1, pp. 295–302, 2012.

[43] M. R. Unnithan, V. P. Vinod, and T. S. Anirudhan, "Synthesis, characterization, and application as a chromium(VI) adsorbent of amine-modified polyacrylamide-grafted coconut coir pith," *Industrial and Engineering Chemistry Research*, vol. 43, no. 9, pp. 2247–2255, 2004.

[44] M. Jain, V. K. Garg, and K. Kadirvelu, "Adsorption of hexavalent chromium from aqueous medium onto carbonaceous adsorbents prepared from waste biomass," *Journal of Environmental Management*, vol. 91, no. 4, pp. 949–957, 2010.

[45] F. Gode and E. Pehlivan, "Removal of Cr(VI) from aqueous solution by two Lewatit-anion exchange resins," *Journal of Hazardous Materials*, vol. 119, no. 1–3, pp. 175–182, 2005.

[46] P. A. Kumar, S. Chakraborty, and M. Ray, "Removal and recovery of chromium from wastewater using short chain polyaniline synthesized on jute fiber," *Chemical Engineering Journal*, vol. 141, no. 1–3, pp. 130–140, 2008.

[47] F. Hussein, "Photochemical treatments of textile industries wastewater," in *Advance in Treating Textile Effluent*, P. J. Hauser, Ed., pp. 117–144, InTech, 2010.

[48] M. R. Samarphandi, M. Zarrabi, M. N. sepehr, A. Amrane, G. H. Safari, and S. Bashiri, "Application of acidic treated pumice as an adsorbent for the removal of azo dye from aqueous solution: kinetic, equilibrium and thermodynamic studies," *Environmental Health Science and Engineering*, vol. 9, no. 5, pp. 1–10, 2012.

[49] N. Ghasemi, S. Mirali, M. Ghasemi, S. Mashhadi, and M. H. Tarraf, "Adsorption isotherms and kinetics studies for the removal of Pb(II) from aqueous solutions using low-cost adsorbent," in *Proceedings of the International Conference on Environment Science and Engineering (IPCBEE '12)*, vol. 32, pp. 79–83, 2012.

[50] Y. S. Ho and G. McKay, "Pseudo-second order model for sorption processes," *Process Biochemistry*, vol. 34, no. 5, pp. 451–465, 1999.

[51] B. Osman, A. Kara, and N. Beşirli, "Immobilization of glucoamylase onto lewis metal ion chelated magnetic affinity sorbent: kinetic, isotherm and thermodynamic studies," *Journal of Macromolecular Science A: Pure and Applied Chemistry*, vol. 48, no. 5, pp. 387–399, 2011.

[52] F. B.-O. Daoud, S. Kaddour, and T. Sadoun, "Adsorption of cellulase Aspergillus niger on a commercial activated carbon: kinetics and equilibrium studies," *Colloids and Surfaces B: Biointerfaces*, vol. 75, no. 1, pp. 93–99, 2010.

[53] W. Plazinski, W. Rudzinski, and A. Plazinska, "Theoretical models of sorption kinetics including a surface reaction mechanism: a review," *Advances in Colloid and Interface Science*, vol. 152, no. 1-2, pp. 2–13, 2009.

[54] Y. G. Zhao, H. Y. Shen, S. D. Pan, and M. Q. Hu, "Synthesis, characterization and properties of ethylenediamine-functionalized Fe_3O_4 magnetic polymers for removal of Cr(VI) in wastewater," *Journal of Hazardous Materials*, vol. 182, no. 1–3, pp. 295–302, 2010.

[55] S. Kathirvel, H.-S. Chen, C. Su, H.-H. Wang, C.-Y. Li, and W.-R. Li, "Preparation of smooth surface TiO_2 photoanode for

high energy conversion efficiency in dye-sensitized solar cells," *Journal of Nanomaterials*, vol. 2013, Article ID 610964, 6 pages, 2013.

[56] A. Kara, B. Acemioðlu, M. H. Alma, and M. Cebe, "Adsorption of Cr(III), Ni(II), Zn(II), Co(II) ýons onto phenolated wood resin," *Applied Polymer Science*, vol. 101, pp. 2838–2846, 2006.

[57] A. Üçer, A. Uyanık, and Ş. F. Aygün, "Adsorption of Cu (II), Cd(II), Zn(II), Mn(II) and Fe(III) ions by tannic acid immobilised activated carbon," *Journal of Separation and Purification Technology*, vol. 47, pp. 113–118, 2006.

[58] G. Asgari, B. Roshani, and G. Ghanizadeh, "The investigation of kinetic and isotherm of fluoride adsorption onto functionalize pumice stone," *Journal of Hazardous Materials*, vol. 217-218, pp. 123–132, 2012.

[59] C. Namasivayam and D. Kavitha, "Removal of congo red from water by adsorption onto activated carbon prepared from coir pith, an agricultural solid waste," *Dyes and Pigments*, vol. 54, no. 1, pp. 47–58, 2002.

[60] M. Doğan, M. Alkan, and Y. Onganer, "Adsorption of methylene blue from aqueous solution onto perlite," *Water, Air, and Soil Pollution*, vol. 120, no. 3-4, pp. 229–248, 2000.

[61] A. Kara, L. Uzun, N. Beşirli, and A. Denizli, "Poly(ethylene glycol dimethacrylate-n-vinyl imidazole) beads for heavy metal removal," *Journal of Hazardous Materials*, vol. 106, no. 2-3, pp. 93–99, 2004.

[62] E. Kalkan, H. Nadaroğlu, N. Celebi, and G. Tozsin, "Removal of textile dye reactive black 5 from aqueous solution by adsorption on laccase-modified silica fume," *Desalination and Water Treatment*, 2013.